

Comparison of three multichannel transmit/receive radiofrequency coil configurations for anatomic and functional cardiac MRI at 7.0T: implications for clinical imaging

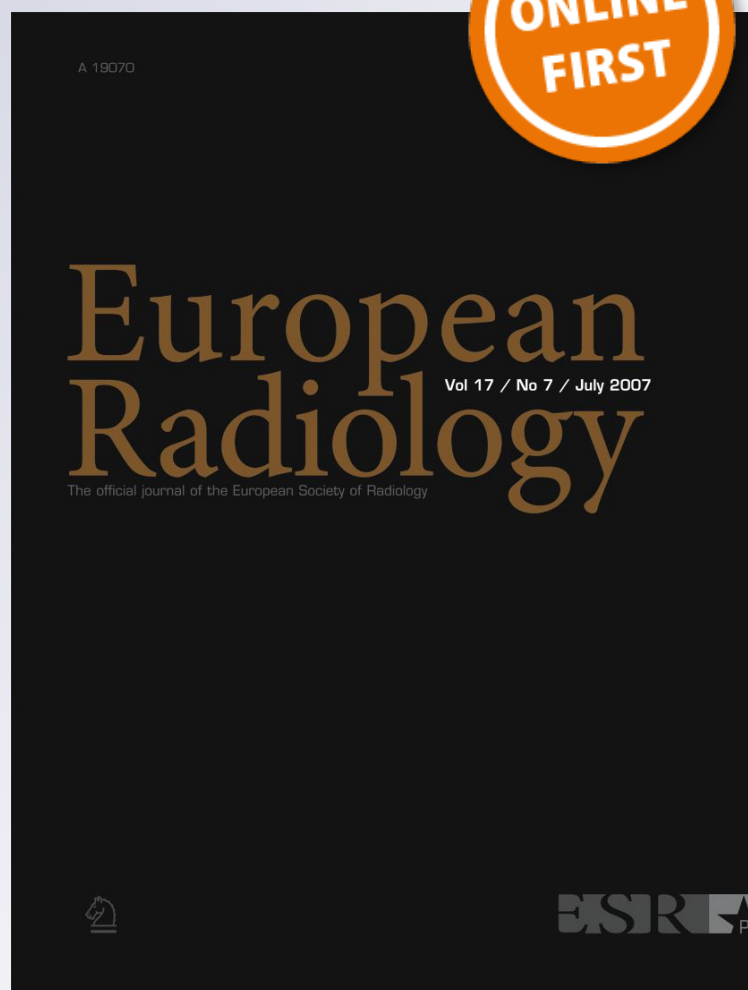
Lukas Winter, Peter Kellman, Wolfgang Renz, Andreas Gräßl, Fabian Hezel, Christof Thalhammer, Florian von Knobelsdorff-Brenkenhoff, et al

European Radiology

ISSN 0938-7994

Eur Radiol

DOI 10.1007/s00330-012-2487-1



Your article is protected by copyright and all rights are held exclusively by European Society of Radiology. This e-offprint is for personal use only and shall not be self-archived in electronic repositories. If you wish to self-archive your work, please use the accepted author's version for posting to your own website or your institution's repository. You may further deposit the accepted author's version on a funder's repository at a funder's request, provided it is not made publicly available until 12 months after publication.

Comparison of three multichannel transmit/receive radiofrequency coil configurations for anatomic and functional cardiac MRI at 7.0T: implications for clinical imaging

Lukas Winter · Peter Kellman · Wolfgang Renz ·
Andreas Gräßl · Fabian Hezel · Christof Thalhammer ·
Florian von Knobelsdorff-Brenkenhoff ·
Valeriy Tkachenko · Jeanette Schulz-Menger ·
Thoralf Niendorf

Received: 16 January 2012 / Revised: 6 April 2012 / Accepted: 10 April 2012
© European Society of Radiology 2012

Abstract

Objectives To implement, examine, and compare three multichannel transmit/receive coil configurations for cardiovascular MR (CMR) at 7T.

Methods Three radiofrequency transmit-receive (TX/RX) coils with 4-, 8-, and 16-coil elements were used. Ten healthy

volunteers (seven males, age 28 ± 4 years) underwent CMR at 7T. For all three RX/TX coils, 2D CINE FLASH images of the heart were acquired. Cardiac chamber quantification, signal-to-noise ratio (SNR) analysis, parallel imaging performance assessment, and image quality scoring were performed.

Results Mean total examination time was 29 ± 5 min. All images obtained with the 8- and 16-channel coils were diagnostic. No significant difference in ejection fraction (EF) ($P > 0.09$) or left ventricular mass (LVM) ($P > 0.31$) was observed between the coils. The 8- and 16-channel arrays yielded a higher mean SNR in the septum versus the 4-channel coil. The lowest geometry factors were found for the 16-channel coil (mean \pm SD 2.3 ± 0.5 for $R=4$). Image quality was rated significantly higher ($P < 0.04$) for the 16-channel coil versus the 8- and 4-channel coils.

Conclusions All three coil configurations are suitable for CMR at 7.0T under routine circumstances. A larger number of coil elements enhances image quality and parallel imaging performance but does not impact the accuracy of cardiac chamber quantification.

Key Points

- Cardiac chamber quantification using 7.0T magnetic resonance imaging is feasible.
- Examination times for cardiac chamber quantification at 7.0T match current clinical practice.
- Multichannel transceiver RF technology facilitates improved image quality and parallel imaging performance.
- Increasing the number of RF channels does not influence cardiac chamber quantification.

L. Winter · W. Renz · A. Gräßl · F. Hezel · C. Thalhammer ·
F. von Knobelsdorff-Brenkenhoff · J. Schulz-Menger ·
T. Niendorf (✉)
Berlin Ultrahigh Field Facility,
Max-Delbrück Center for Molecular Medicine,
Robert-Roessle-Strasse 10,
13125 Berlin, Germany
e-mail: Thoralf.Niendorf@mdc-berlin.de

F. von Knobelsdorff-Brenkenhoff · J. Schulz-Menger
Department of Cardiology and Nephrology,
HELIOS Klinikum Berlin-Buch,
Berlin, Germany

F. von Knobelsdorff-Brenkenhoff · V. Tkachenko ·
J. Schulz-Menger · T. Niendorf
Experimental and Clinical Research Center,
A joint cooperation between the Charité Medical Faculty
and the Max-Delbrück Center for Molecular Medicine,
Berlin, Germany

P. Kellman
Laboratory of Cardiac Energetics,
National Institutes of Health/NHLBI,
Bethesda, MD, USA

W. Renz
Siemens Healthcare,
Erlangen, Germany

Keywords Ultra-high field MRI · Cardiovascular MRI · Transceiver array · Parallel imaging · Cardiac chamber quantification

Introduction

Cardiac magnetic resonance (CMR) imaging at ultra-high fields (UHF) is regarded as one of the most challenging MRI applications since it is accompanied by various technical difficulties [1–11]. In UHF CMR image quality is not always exclusively defined by signal-to-noise ratio (SNR) and contrast-to-noise ratio (CNR)

gains inherent in UHF. Although UHF CMR is still in its infancy, recent reports have demonstrated that cardiac chamber quantification at 7T is feasible and matches left ventricular (LV) parameters derived from 1.5T and 3T acquisitions [7, 8, 11, 12].

These developments are supported by explorations into novel radiofrequency (RF) technology including multichannel transmit/receive (TX/RX) RF coil arrays comprising various coil designs [1, 2, 13, 14]. This approach helps to overcome some of the transmit B_1 -field heterogeneity and image quality constraints present at 7T. Consequently, TX/RX arrays are a requirement for UHF CMR. Realizing this necessity, this study implements and compares three

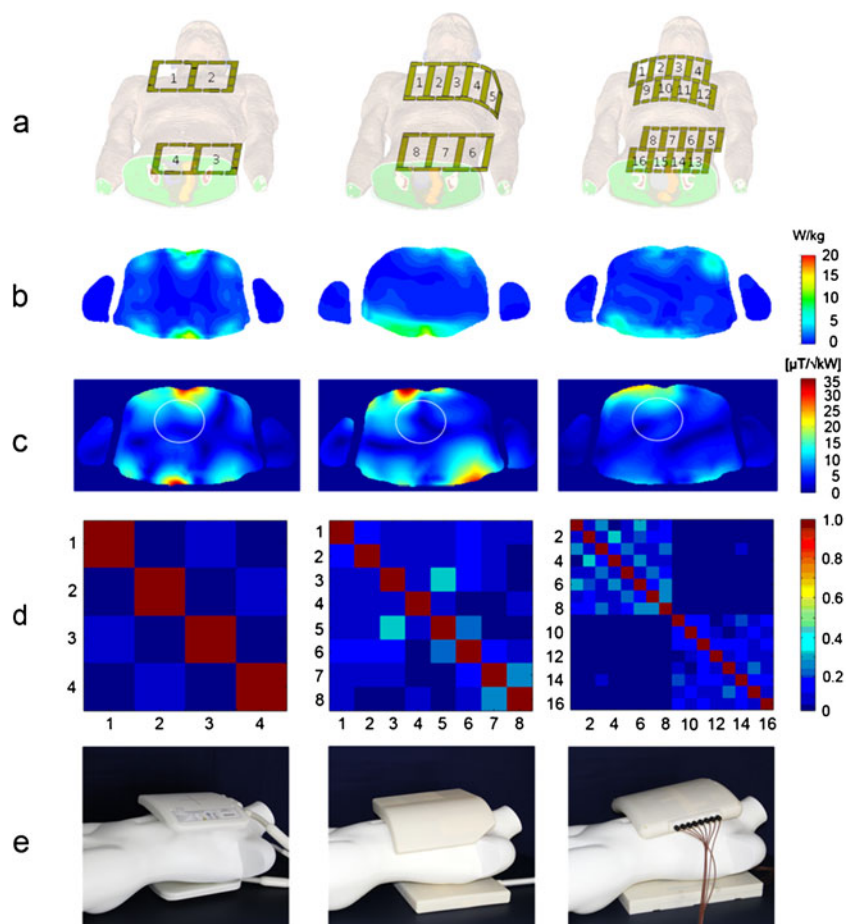


Fig. 1 **a** Basic schemes of the three TX/RX coil designs used in this study: *left* 4-channel TX/RX coil with two anterior and two posterior elements of $13 \times 20 \text{ cm}^2$ (S-I dimension: 20 cm, L-R dimension: 26 cm) [13], *center* 8-channel TX/RX coil with five anterior elements each $6 \times 19 \text{ cm}^2$ plus three posterior elements of $9 \times 19 \text{ cm}^2$ (S-I dimension: 21 cm, L-R dimension: 31 cm) [14], *right* 16-channel TX/RX coil with eight anterior and eight posterior elements of $6 \times 13 \text{ cm}^2$ (S-I dimension: 28 cm, L-R dimension: 29 cm). **b** Simulation of the signal-absorption rate (SAR) distribution (local SAR, 10 g average) for an axial slice for the 4-channel (*left*), 8-channel (*middle*), and 16-channel (*right*) TX/RX coils. The limits for partial body SAR or for maximum local SAR of 20 W/kg given by the IEC [16] were not exceeded. **c** Simulation of the transmit field efficiency

($B_1^+/\sqrt{P_{\text{delivered}}}$) in a mid-axial view of the 4-channel (*left*), 8-channel (*middle*), and 16-channel (*right*) TX/RX coils. The white ROI indicates the position of the heart. **d** Normalized noise correlation matrices averaged over 10 subjects for the 4-channel (*left*), 8-channel (*middle*), and 16-channel (*right*) TX/RX coils, which indicate descent decoupling between coil elements. The maximum noise correlation was 0.11 ± 0.04 for the 4-channel coil, 0.25 ± 0.05 for the 8-channel coil, and 0.19 ± 0.02 for the 16-channel coil. **e** Photographs of the 4-channel (*left*), 8-channel (*middle*), and 16-channel (*right*) TX/RX coil to illustrate the coil design and the geometry of the coil casing together with the coil positioning used in a clinical setting

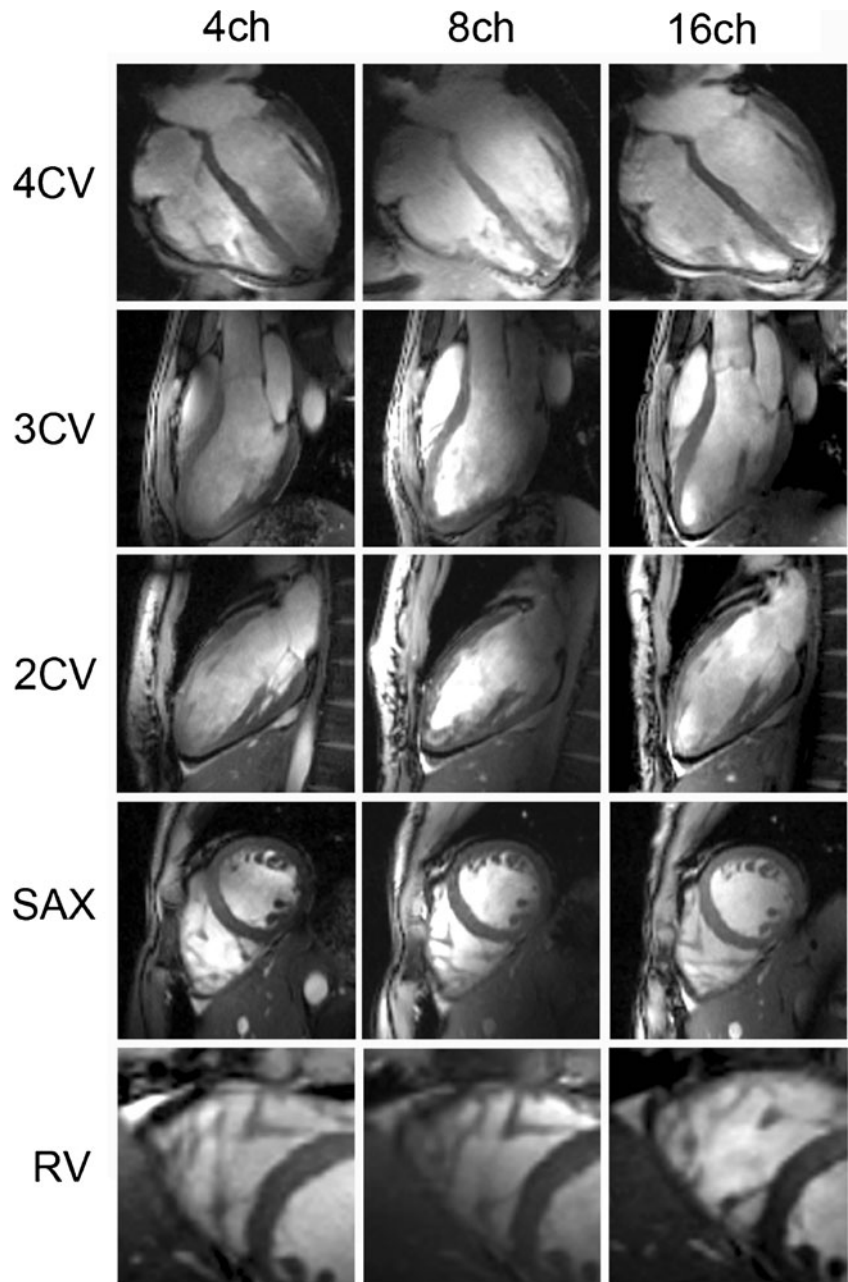
Table 1 Survey of transmit phases used for the 4-channel, 8-channel, and 16-channel coils. Element numbering is indicated in Fig. 1

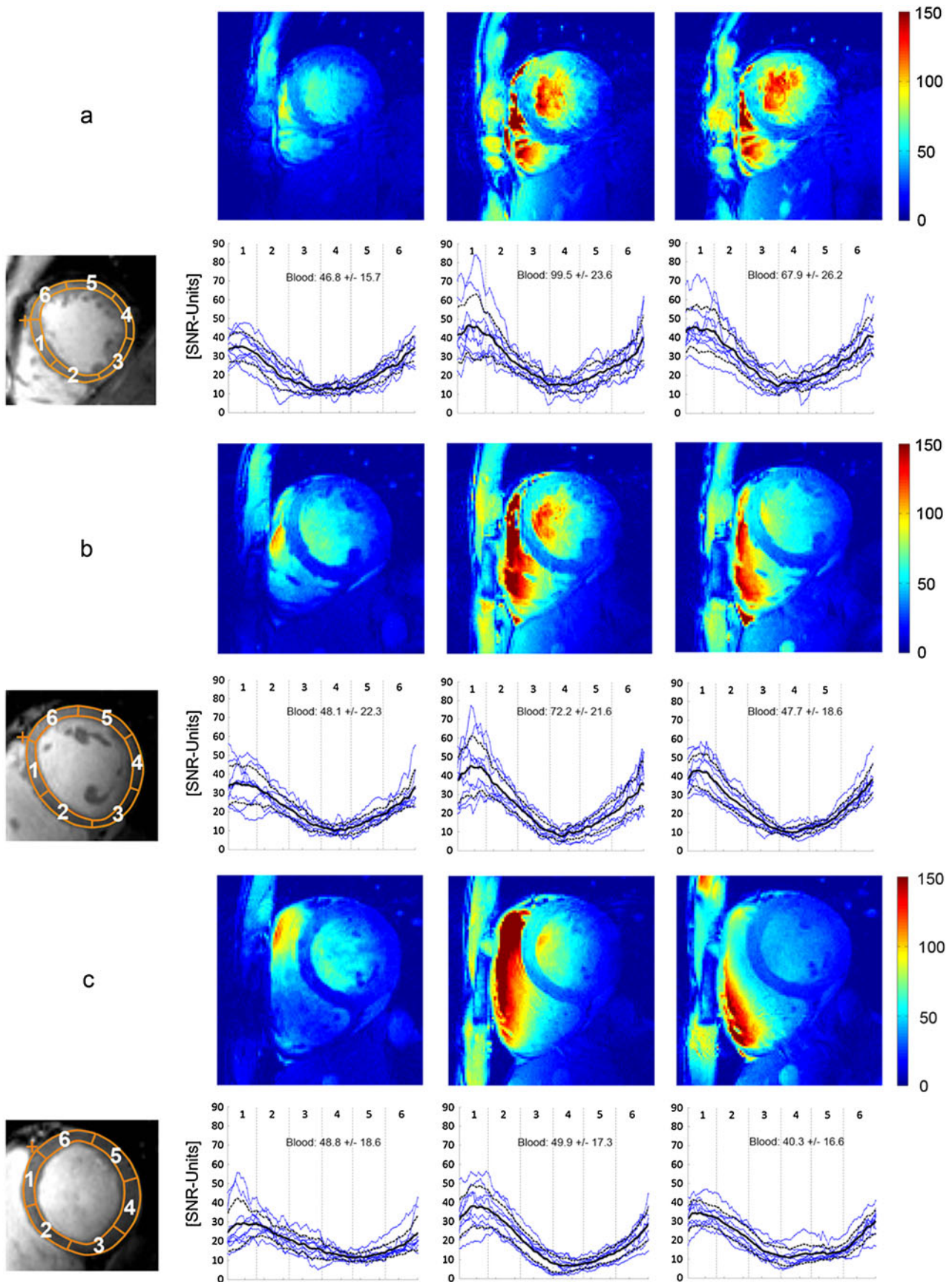
Channel	1	2	3	4	5	6	7	8	9	10	11	12	13	14	15	16
4ch	225	45	180	0	-	-	-	-	-	-	-	-	-	-	-	-
8ch	315	0	135	130	245	0	30	60	-	-	-	-	-	-	-	-
16ch	0	23	45	68	180	203	225	248	11	34	56	79	191	214	236	259

multichannel TX/RX RF coils tailored for UHF CMR and examines their applicability at 7T in a routine setting. The coil comparison comprises safety evaluation, image quality assessment, SNR and CNR analysis, examination of parallel

imaging performance, and cardiac chamber quantification. The merits and limitations of the arrays are discussed, and implications for cardiac MR at 7T are considered in this technical development note.

Fig. 2 2D CINE FLASH images for the 4-channel (*left*), 8-channel (*middle*), and 16-channel (*right*) TX/RX coil arrays derived from the same subject. A four-chamber view (4CV), three-chamber view (3CV), two-chamber view (2CV), short-axis view (SAX), and a magnified view of subtle anatomic details of the right ventricle (RV) at end-diastole are displayed. The images were not corrected for receive inhomogeneity. The image quality scores for the displayed images are as follows: 4CV 4-ch diastole=2; 4CV 8-ch diastole=2; 4CV 16-ch diastole=3; 3CV 4-ch diastole=2; 3CV 8-ch diastole=2; 3CV 16-ch diastole=3; 2CV 4-ch diastole=3; 2CV 8-ch diastole=3; 2CV 16-ch diastole=3; SAX 4-ch diastole=3; SAX 8-ch diastole=3; SAX 16-ch diastole=3





◀ **Fig. 3** Quantitative signal-to-noise ratio (SNR) maps ($R=2$) and mean SNR value graphs observed at end-diastole for the 4-channel coil (*left*), 8-channel coil (*middle*), and 16-channel coil (*right*) for **a** an apical short-axis view, **b** a midventricular short-axis view, and **c** a basal short-axis view. The *blue lines* indicate the SNR distribution across the six segments of the myocardium for all subjects. The *black line* represents the mean SNR value over all subjects. Mean and standard deviation of SNR of the left ventricular blood pool are annotated in the graphs for all three slice positions

Materials and methods

Subjects

The study was performed with the approval of the local ethics committee. All subjects gave written informed consent prior to the study. Ten volunteers [seven males; mean \pm standard deviation (SD) age 27.5 ± 4.1 years, range 24–38 years; mean \pm SD body mass index 21.4 ± 2.8 kg/m², range 18.4–26.8 kg/m²] underwent CMR. All subjects were in normofrequent sinus rhythm (mean heart rate 67 ± 7 bpm).

MR and RF coil technology

Four-channel [13], 8-channel [14], and 16-channel TX/RX coils that use loop elements were implemented (Fig. 1). The 4-channel TX/RX coil exhibits two anterior and two posterior elements each arranged in a one-dimensional array. The 8-channel TX/RX coil comprises five anterior elements each arranged in a one-dimensional array. The 16-channel TX/RX coil involves eight anterior and eight posterior elements each laid out on a 2×4 two-dimensional grid, which improves receive acceleration in two dimensions.

The mean values for the ratios of Q_u (Q-factor unloaded) over Q_L (Q-factor loaded by a volunteer) were $Q_{4ch} = 7.0/7.0$, $Q_{8ch} = 6.5/11.4$, and $Q_{16ch} = 4.3/4.3$ for the anterior/posterior coil elements. The reflection coefficients were below -13 dB for the 4-channel coil, -14 dB for the 8-channel coil, and -16 dB for the 16-channel coil, and the transmission coefficients were below -15 dB for the 4-channel coil, -12 dB for the 8-channel coil, and -13 dB for the 16-channel coil for all coil elements and volunteers. Imaging was performed on a 7T whole-body MR system (Magnetom, Siemens Healthcare, Erlangen, Germany). The output of an 8 kW RF amplifier (Stolberg HF Technik, Stolberg-Vicht, Germany) was split into 4, 8, or 16 channels—each with equal signal intensity—by means of a home-built splitter box and additional cables used for phase shifting. The coil arrays were connected to the MR system via a coil interface comprising 4, 8, or 16 TX/RX switches and low-noise preamplifiers (Stark Contrasts, Erlangen, Germany). Phase settings of the transmit channels were adjusted as described in [14] to improve uniformity of RF transmission (B_1^+) and of

blood/myocardium contrast. The transmit phase calculations were based on B_1^+ profiles derived from numerical field simulations (CST Microwave Studio, Darmstadt, Germany) and the voxel model “Duke” from the Virtual Family [15]. The EMF simulations were validated against MR measurements using an elliptical phantom filled with a dielectric liquid ($\epsilon_r = 57.8$, $\sigma = 0.78$ S/m). For this, relative B_1^+ distributions of the individual coil elements derived from the EMF simulations were compared to B_1^+ maps acquired with the double angle method. The transmit phases for each coil element were adjusted using iterative algorithms (pTX PulseDesign Suite, Siemens Healthcare, Erlangen, Germany) to improve field homogeneity in an ROI encompassing an axial view of the heart. All coils were operated with this fixed phase setting (Table 1) throughout the volunteer study.

To achieve flip angles at 7T that support high blood/myocardium contrast while not putting the subject at any risk, numerical specific absorption rate (SAR) (10 g average) simulations were performed with all coils and the voxel model Duke. The power settings for all coils were based on careful examinations of the partial body and local SAR values according to the IEC guidelines [16].

Imaging protocol

All volunteers were examined with all three coils. For retrospective gating an MR stethoscope (EasyACT, MRI.Tools, Berlin, Germany) was used [17, 18]. Images were acquired using a 2D CINE FLASH technique [FOV 360×326 mm², TE 2.7 ms, TR 5.6 ms, receiver bandwidth 444 Hz/px, volume selective B_0 shimming, 30 cardiac phases, temporal resolution 33 ms (heart rate of 60 bpm), 8 views per segment, slice thickness 4 mm [7], slice gap 2 mm, data acquisition/reconstruction matrix size $256 \times 232/256 \times 256$ elements, spatial resolution $1.4 \times 1.4 \times 4$ mm³, nominal flip angle $\alpha 35^\circ$, transmit reference voltage U_{ref} 400 V, peak voltage of sinc-pulse ($t = 800$ μ s) U_{peak} 190 V]. Image acquisition was confined to a single slice per end expiratory breath-hold. Parallel imaging was performed for short-axis views using GRAPPA (32 calibration lines) [19] with reduction factors of $R=1, 2, 3, 4$ resulting in acquisition times of 36 s ($R=1$), 22 s ($R=2$), 17 s ($R=3$), and 4 s ($R=4$) for a heart rate of 60 bpm. All other views were acquired with $R=2$. For each subject, two-, three-, and four-chamber standard views of the left ventricle and a set of short-axis views ranging from the atrioventricular ring to the apex were acquired.

Image quality assessment

For SNR/CNR assessment, basal, midventricular, and apical short-axis views were scaled in SNR units [20]. For

this purpose the 2D CINE FLASH technique included a preliminary noise sequence to measure the noise-correlation matrix [20]. Standardized segmentation of the heart [21] was applied to the end-systolic and end-diastolic cardiac phases (QMass MR, Medis Medical Imaging Systems, Leiden, Netherlands). Overall image quality was scored in a blinded consensus reading of two experienced CMR readers based on blood/myocardium contrast, anatomic border sharpness, and visualization of subtle anatomical features (such as ventricular trabeculae) using a scale [7] ranging from 0 to 3 (0=nondiagnostic, 1=impaired image quality that may lead to misdiagnosis, 2=good, 3=excellent).

For analysis of parallel imaging performance, geometry factor (g-factor) maps were calculated [20] for all reduction factors using basal, midventricular, and apical short-axis slices and evaluated for a region of interest (ROI) encompassing the heart.

Cardiac chamber quantification

For LV chamber quantification, end-diastolic and end-systolic volume (EDV, ESV), LV ejection fraction (EF), and left ventricular mass (LVM) were obtained by manually contouring the endocardial and epicardial borders in end-diastole and end-systole (CMR42[®], Circle Cardiovascular Imaging, Calgary, Canada) using images derived from two-fold accelerated acquisitions. Blinded CMR reading was performed by two clinicians with expertise in clinical CMR (>3,000 CMR examinations), who were not involved in the image acquisition.

Statistical analysis

Differences in the data derived from the 4-, 8-, and 16-channel coils were analyzed using Wilcoxon signed rank test for image quality and *t*-test for chamber quantification. A *P*-value of <0.05 was regarded as significant.

Results

RF coil design, RF coil characteristics, and RF safety evaluation

The RF safety assessment based on simulations for the voxel model Duke revealed that RF power deposition did not exceed a partial body SAR of 1.4 W/kg, (4-channel coil: 1.4 W/kg, 8-channel coil: 1.0 W/kg, 16-channel coil: 0.7 W/kg) for the phase settings used. The SAR levels fall well within the limits of the IEC guidelines [16]. Calculations of the local SAR (10 g average), as illustrated in Fig. 1b, indicated local maxima below 20 W/kg (4-channel coil: 17 W/kg,

8-channel coil: 13 W/kg, 16-channel coil: 11 W/kg) for an input power of $P_{in}=30$ W, which defines the threshold for operation in the first level mode [16]. The simulations provide limited insight into local SAR distributions as the transmitted field of the coils and consequently SAR at 7T vary substantially with typical anatomical differences among subjects as well as with coil positioning. Consequently the simulation-based local SAR contributions have to be applied conservatively in practice. Averaged transmit field efficiency over an ROI encompassing a mid-axial view of the heart was found to be $7.4\pm 3.6 \mu T/\sqrt{kW}$ (4-channel), $5.4\pm 3.1 \mu T/\sqrt{kW}$ (8-channel), and $6.5\pm 3.1 \mu T/\sqrt{kW}$ (16-channel) as depicted in Fig. 1c.

Noise correlation between coil elements was measured in-vivo and averaged over all subjects. The resulting matrices are shown in Fig. 1d and indicate a rather low noise correlation. The maximum noise correlation was 0.11 ± 0.04 for the 4-channel coil, 0.25 ± 0.05 for the 8-channel coil, and 0.19 ± 0.02 for the 16-channel coil.

All coils used shaped, lightweight configurations that fit to the anterior chest (Fig. 1e) without compromising the subject's comfort or the ease of use. The anterior coils exhibit a weight and curvature of 1.35 kg, 1,800 mm radius, 9° angle for the 4-channel coil; 2.1 kg, 130 mm radius, 35° angle for 8-channel coil; and 2.3 kg, 313 mm radius, 55° angle for the 16-channel coil. In comparison, a commercially available and clinically established 32-channel RX coil tailored for cardiac MRI (In vivo, Gainesville, FL) exhibits a weight of 2.7 kg for the anterior section.

Image quality assessment

All coil configurations provided whole heart coverage as shown in Fig. 2. All subjects tolerated all examinations well without adverse events. The mean total examination time, including a localizer scan, four standard cardiac views, and a set of 21 short-axis view slices covering the entire LV using two-fold accelerated acquisitions, was found to be 29 ± 5 min. For the acquisition of the short-axis view stack, a mean examination time of 16 ± 3 min was observed.

2D CINE FLASH imaging provided excellent blood/myocardium contrast for all examined slice orientations. Figure 2 depicts four-, three-, and two-chamber long-axis views, and a midventricular short-axis view of the heart.

SNR and CNR values are surveyed in Fig. 3. The mean SNR values are depicted in Table 2. All short-axis views revealed an SNR gradient from the septum towards the lateral wall. The 8-channel and 16-channel arrays yielded a higher mean SNR in the septum (segments 1–2) versus the 4-channel coil. For comparison, the SNR of the lateral wall provided similar values for each coil. The overall signal homogeneity was found to be the best for the 4-channel

Table 2 Survey of the results derived from the signal-to-noise ratio (SNR) analysis. Mean SNR values are shown for all three RF coils using parallel imaging reduction factors ranging from R=1 to R=4 for

Reduction factor (R) used for parallel imaging	4-channel TX/RX coil		8-channel TX/RX coil		16-channel TX/RX coil	
	Anteroseptal mid-cavity	Inferolateral mid-cavity	Anteroseptal mid-cavity	Inferolateral mid-cavity	Anteroseptal mid-cavity	Inferolateral mid-cavity
R=1	77	34	96	29	77	28
R=2	41	18	57	17	50	18
R=3	24	9	29	8	30	11
R=4	21	8	27	6	27	11

the anteroseptal mid-cavity (segment 8) and the inferolateral mid-cavity (segment 11) of short-axis view as described in [21]

array indicated by the smallest gradient in the SNR values across the entire heart as well as the blood pool. For the anteroseptal segment of the mid-ventricular slice a blood/myocardium CNR of 22 was found for the 4-channel coil. The 8-channel coil showed a CNR of 33 while the 16-channel coil provided a CNR of 18. For the anterolateral segment of the mid-ventricular slice, a blood/myocardium CNR of 52 was found for the 4-channel coil. The 8-channel coil showed a CNR of 71 while the 16-channel coil provided a CNR of 54.

The image quality scoring revealed that all datasets derived from the 8- and 16-channel coils were found to be diagnostic. One dataset acquired with the 4-channel array was rated to be nondiagnostic. This was attributed to the lack of sufficient blood/myocardium contrast in one apical short-axis view. Significant differences in LV image quality were found between (1) the 16-channel ($P=0.037$) and the 4-channel coils and (2) between the 8-channel ($P=0.005$) and the 16-channel coils (Fig. 4). The 16-channel TX/RX coil produced the best image quality, which was significantly improved versus the 8-channel TX/RX coil (P -values: end-diastole: $P=0.01$, end-systole: $P=0.05$) and versus the 4-channel coil (P -values: end-diastole: $P=0.04$, end-systole: $P<0.01$). End-systolic LV overall image quality was rated 2.28 ± 0.12 for the 16-channel coil, 2.14 ± 0.28 for the 8-channel coil, and 1.77 ± 0.31 for the 4-channel coil. End-diastolic LV overall image quality was rated 2.3 ± 0.24 for the 16-channel coil, 1.82 ± 0.31 for the 8-channel coil, and 1.91 ± 0.37 for the 4-channel coil. The image quality rating (end-systole/end-diastole) for the right ventricle (RV) was $2.28\pm 0.28/2.35\pm 0.23$ for the 16-channel coil, $2.19\pm 0.27/1.93\pm 0.25$ for the 8-channel coil, and $1.72\pm 0.44/1.88\pm 0.35$ for the 4-channel coil.

A synopsis of the analysis of the parallel imaging data sets together with the g-factor maps is shown in Fig. 5a, b. Parallel imaging revealed lowest noise amplification for the 16-channel array for all acceleration factors used as shown in Fig. 5c. The noise amplification obtained for the 4-channel coil makes the use of acceleration factors larger than R=2 almost prohibitive for diagnostic imaging (Fig. 5c). In

comparison, the 16- and 8-channel coils provided image quality that is clinically acceptable for R=3 and R=4.

Cardiac chamber quantification

The mean quantitative LV results (R=2) are depicted in Fig. 6. No significant difference was found for EF/LVM (1) between the 8-channel ($P=0.59/P=0.31$) and 16-channel ($P=0.15/P=0.58$) versus the 4-channel coil and (2) between the 8-channel ($P=0.16/P=0.35$) versus the 16-channel coil. Mean values over all volunteers are shown in Table 3.

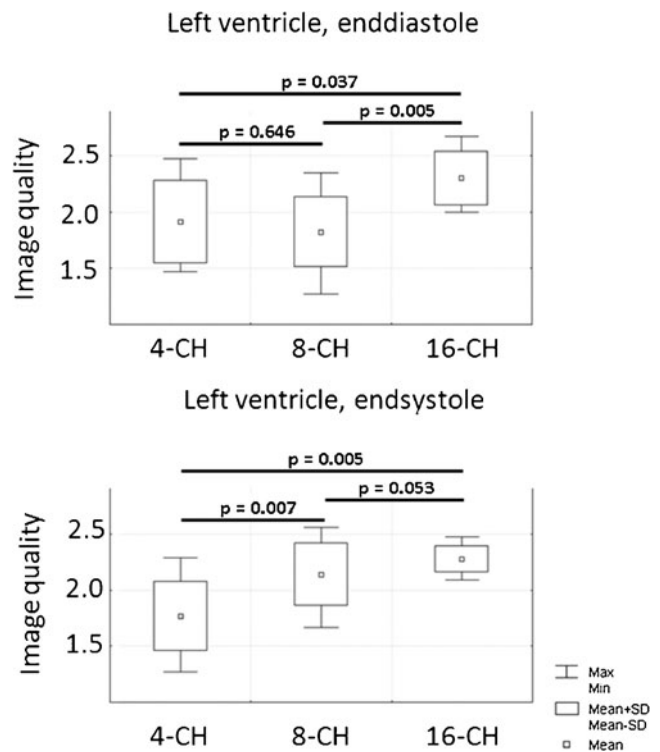


Fig. 4 Left ventricular image quality scores derived from a blinded consensus reading including two experienced clinicians. For image quality scoring, a scale [7] ranging from 0 to 3 (0=nondiagnostic; 1=impaired image quality that may lead to misdiagnosis; 2=good; 3=excellent) was used

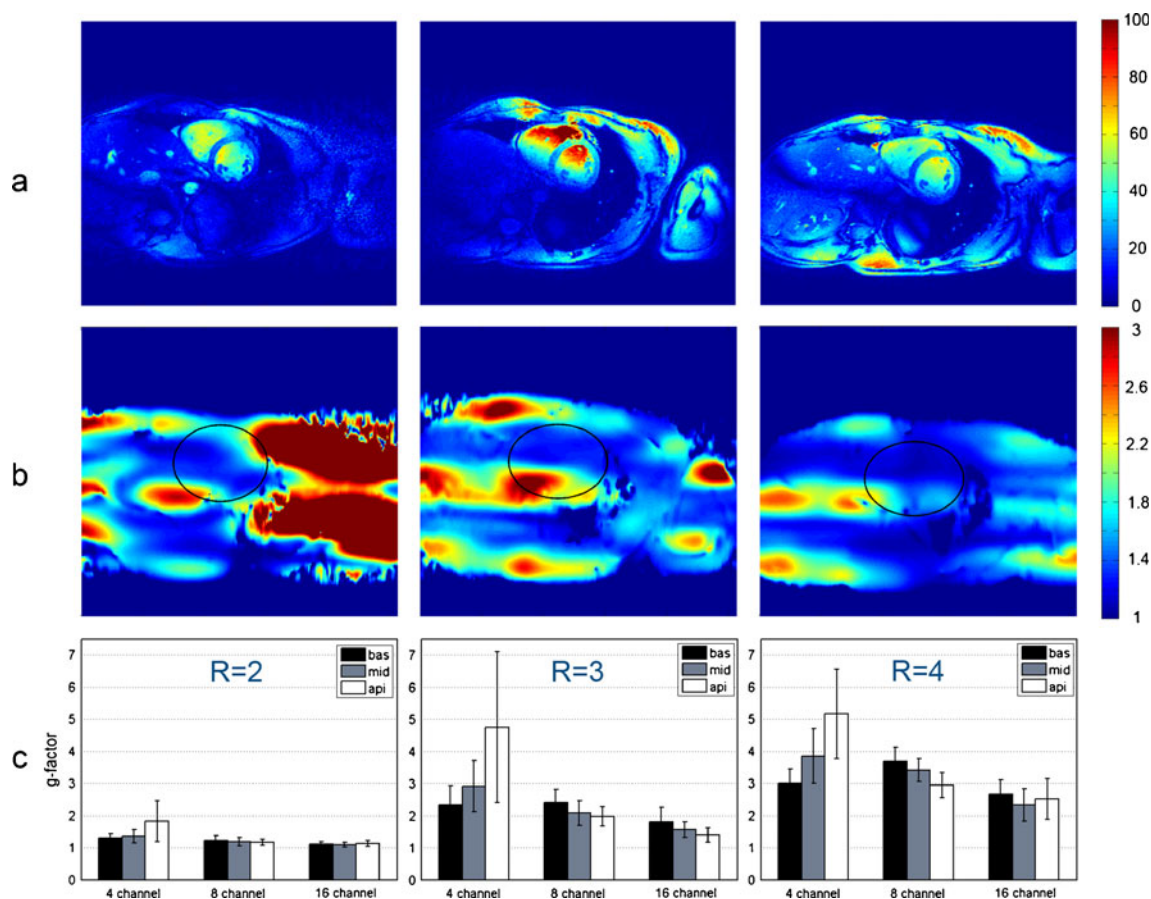


Fig. 5a–c Survey of the parallel imaging performance of the 4-channel, 8-channel, and 16-channel TX/RX coil. **a** Quantitative signal-to-noise ratio (SNR) maps observed for GRAPPA reconstruction using an acceleration factor of R=4 for the 4-channel (*left*), the 8-channel (*middle*), and the 16-channel TX/RX (*right*) coil. **b** Geometry factor (g-factor) maps derived from GRAPPA reconstruction for an acceleration factor of R=4 for the 4-channel (*left*), the 8-channel (*middle*), and the 16-channel (*right*) TX/RX coil with a region-of-interest (ROI) indicating the position of the heart. **c** Comparison of g-factor (mean value and standard deviation) obtained for the 4-, 8-, and 16-channel TX/RX coils for *left* basal (bas), *middle* midventricular (mid), and *right* apical (api) short-axis views. For midventricular

short-axis views derived from the 16-channel array, mean g-factors of 1.10 ± 0.07 (R=2), 1.57 ± 0.24 (R=3), and 2.33 ± 0.5 (R=4) were obtained. For comparison the 8-channel coil showed mean g-factors of 1.19 ± 0.13 (R=2), 2.08 ± 0.39 (R=3), and 3.41 ± 0.35 (R=4). The 4-channel coil yielded g-factors of 1.35 ± 0.20 (R=2), 2.92 ± 0.79 (R=3), and 3.85 ± 0.85 (R=4). Noise amplification due to the use of parallel imaging decreases as the number of TX/RX channels increases. The 16-channel TX/RX showed less parallel imaging-induced noise amplification than the 8-channel and the 4-channel TX/RX coils. The noise amplification performance of the 4-channel TX/RX coil renders it unsuitable for acceleration factors larger than R=2

Discussion

This technical development note demonstrates that a larger number of elements in conjunction with a two-dimensional array design can improve image quality as well as parallel imaging performance. 2D CINE imaging yielded clinically acceptable image quality for all coil designs used here including rather uniform intensities across the heart with SNR and myocardium/blood contrast that can compete with those of clinical 2D CINE SSFP imaging established at 1.5T. These results were obtained while also achieving a spatial resolution that is superior by a factor of three or more to what is been commonly applied in clinical CMR protocols used for LV function assessment [8]. Taking the enhanced spatial resolution and the increased number of slices into account, the

examination times compare very well with LV function assessment protocols commonly used at 1.5 or 3T. Since static phase setting and RF coil adjustments are used, no extra scan time penalty per slice is introduced at 7.0T, while spatial resolution and blood myocardium contrast are superior to or competitive with those common at 1.5 and 3.0T. If patient-specific B_1^+ shimming and extra coil adjustments are applied, averaged total examination times are substantially prolonged and can lengthen towards averaged total examination times of 93 min [11], which exceeds what is clinically acceptable.

Previous authors have used a single-loop element or a four-loop element TX/RX coil for cardiac chamber quantification at 7.0T [7] including a comparison with SSFP imaging at 1.5T, which is the current gold standard for LV function assessment. Our study adds to the current literature

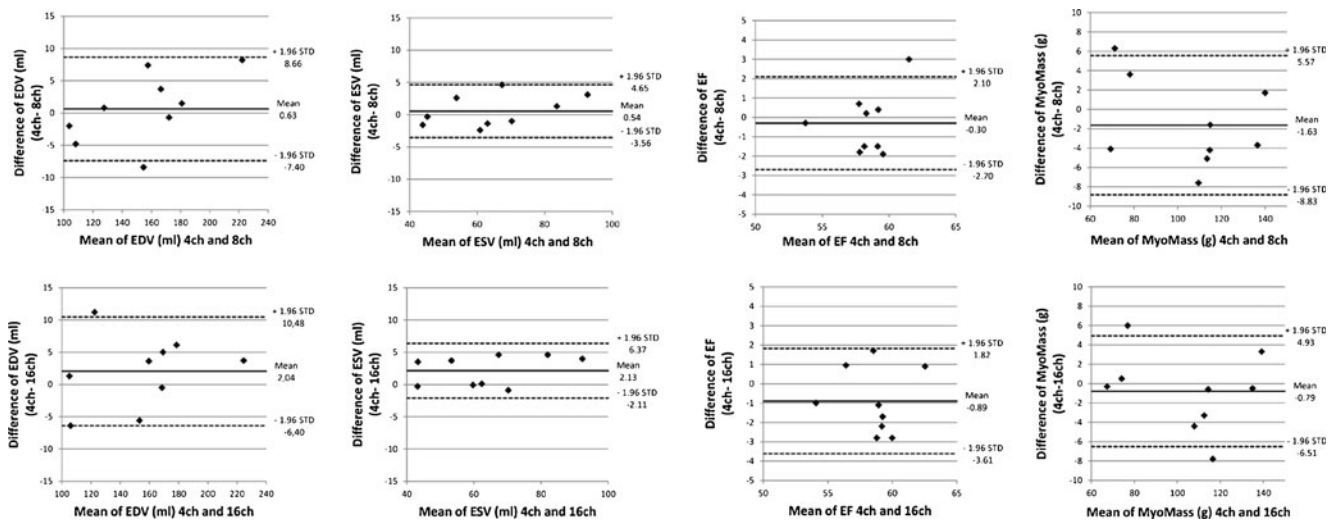


Fig. 6 Bland-Altman plots of the results derived from cardiac chamber quantification including end-diastolic volume (EDV), end-systolic volume (ESV), ejection fraction (EF), and LV myocardial mass (LVM). The 8-channel (8ch) and 16-channel (16ch) TX/RX coil were

benchmarked against the 4-channel (4ch) coil, which was used as a reference. For EF and LVM, no significant differences were found between the 8-channel TX/RX coil and the 16-channel TX/RX coil versus the 4-channel TX/RX coil

by demonstrating that, compared to a single-loop element and a 4-channel TX/RX coil, the use of an 8- or 16-channel TX/RX loop element coil is as accurate in cardiac chamber quantification at 7.0T. The larger number of elements enhances the image quality for the left and right ventricles across the heart and offers a speed advantage due to the improved parallel imaging performance. The noise amplification performance of the 4-channel TX/RX coil renders it unsuitable for acceleration factors larger than $R=2$. The 16-element coil array showed a performance that was superior to that of the 4- and 8-element coil arrays. With supporting acceleration factors of up to four, the 16-channel coil array design offers scan accelerations that would be beneficial for acquisition of multiple slices per breath-hold. This approach would facilitate further reduction of total scan times and offers the potential to streamline cardiac chamber quantification.

It is a recognized limitation of this technical development study that B_1^+ calibration is limited to accomplishing the best blood/myocardium contrast possible, which is the currency for LV assessment in clinical practice. Consequently,

Table 3 Synopsis of the results derived from the cardiac chamber quantification. Mean and SD values of end-diastolic volume (EDV), end-systolic volume (ESV), ejection fraction (EF), and left ventricular mass (LVM) derived from 2D CINE acquisitions of the heart using the 4-channel, 8-channel, and 16-channel TX/RX coil are shown

	4 channel	8 channel	16 channel
EDV (ml)	155.2±39.1	151.8±35.0	150.7±36.5
ESV (ml)	64.8±16.9	63.2±15.3	61.2±16.0
EF (%)	58.2±2.5	58.4±1.9	59.5±2.7
LVM (g)	104.5±25.9	105.1±26.1	104.1±25.6

SNR reported here might be biased by underlying (and spatially varying) B_1^+ differences. B_1^+ calibration could have been performed in stationary tissue adjacent to the heart to circumvent the difficulties of calibrating in the moving heart tissue, though this approach does not necessarily ensure the excellent blood/myocardium contrast that is required for delineation of endo- and epicardial borders.

Our study, while important, indicates the need for additional studies including two-dimensional TX/RX coil arrays with more than 16 elements. This approach would facilitate transmit whole-body arrays at 7.0T and hence would be not only beneficial for CMR but also for body imaging and other large volume MRI applications. A larger number of receive channels would facilitate parallel imaging techniques that provide acceleration required for large-volume 3D acquisitions while achieving a spatial resolution commonly used for routine multislice 2D CINE acquisitions. The maximum possible acceleration increases as the number of array elements increases. Also, multidimensional RF coil arrays are capable of multidimensional accelerations, which serve to reduce noise amplification inherent in parallel imaging and hence preserve SNR as compared to one-dimensional accelerations. 3D volumetric acquisitions also serve to recover SNR via noise averaging [22]. Hence, we anticipate extending our coil designs to configurations suitable for volumetric acquisitions by exploiting 32 or even 64 TX/RX channels, which is beyond the scope of the current work.

In summary, our results (1) indicate that the 16-channel TX/RX coil design is suitable for gaining most uniform, high spatial and temporal resolution CINE images of the heart with diagnostic image quality and largest scan accelerations versus the 4- and 8-channel coil arrays, (2) underline the challenges

of CMR at 7.0T, and (3) demonstrate that these issues can be offset with tailored multichannel RF coils.

References

- Vaughan JT, Snyder CJ, DelaBarre LJ et al (2009) Whole-body imaging at 7T: preliminary results. *Magn Reson Med* 61:244–248
- Snyder CJ, DelaBarre L, Metzger GJ et al (2009) Initial results of cardiac imaging at 7 Tesla. *Magn Reson Med* 61:517–524
- Frauenrath T, Hezel F, Heinrichs U et al (2009) Feasibility of cardiac gating free of interference with electro-magnetic fields at 1.5 Tesla, 3.0 Tesla and 7.0 Tesla using an MR-stethoscope. *Invest Radiol* 44:539–547
- van Elderen SG, Versluis MJ, Webb AG et al (2009) Initial results on in vivo human coronary MR angiography at 7T. *Magn Reson Med* 62:1379–1384
- Versluis MJ, Tsekos N, Smith NB, Webb AG (2009) Simple RF design for human functional and morphological cardiac imaging at 7tesla. *J Magn Reson* 200:161–166
- van Elderen SG, Versluis MJ, Westenberg JJ et al (2010) Right coronary MR angiography at 7T: a direct quantitative and qualitative comparison with 3T in young healthy volunteers. *Radiol* 257:254–259
- von Knobelsdorff-Brenkenhoff F, Frauenrath T, Prothmann M et al (2010) Cardiac chamber quantification using magnetic resonance imaging at 7 Tesla—a pilot study. *Eur Radiol* 20:2844–2852
- Brandts A, Westenberg JJ, Versluis MJ et al (2010) Quantitative assessment of left ventricular function in humans at 7T. *Magn Reson Med* 64:1471–1477
- Frauenrath T, Hezel F, Renz W et al (2010) Acoustic cardiac triggering: a practical solution for synchronization and gating of cardiovascular magnetic resonance at 7 Tesla. *J Cardiovasc Magn Reson* 12:67
- Niendorf T, Sodickson DK, Krombach GA, Schulz-Menger J (2010) Toward cardiovascular MRI at 7T: clinical needs, technical solutions and research promises. *Eur Radiol* 20:2806–2816
- Suttie JJ, Delabarre L, Pitcher A et al (2012) 7 Tesla (T) human cardiovascular magnetic resonance imaging using FLASH and SSFP to assess cardiac function: validation against 1.5T and 3T. *NMR Biomed* 25:27–34
- Maderwald S, Nassenstein K, Orzada S, et al (2010) MR imaging of cardiac wall-motion at 1.5T and 7T: SNR and CNR comparison. *Proc Intl Soc Magn Reson Med* 18:1299
- Dieringer MA, Renz W, Lindel T et al (2011) Design and application of a four-channel transmit/receive surface coil for functional cardiac imaging at 7T. *J Magn Reson* 33:736–741
- Gräbl A, Winter L, Thalhammer C, et al (2011) Design, evaluation and application of an eight channel transmit/receive coil array for cardiac MRI at 7.0T. *Eur J Radiol*. doi:10.1016/j.ejrad.2011.08.002
- Christ A, Kainz W, Hahn EG et al (2010) The Virtual Family—development of surface-based anatomical models of two adults and two children for dosimetric simulations. *Phys Med Biol* 55:N23
- IEC (2010) 60601-2-33 Medical electrical equipment—part 2-33: particular requirements for the basic safety and essential performance of magnetic resonance equipment for medical diagnosis, ed 3.0. International Electrotechnical Commission, Geneva
- Frauenrath T, Niendorf T, Kob M (2008) Acoustic method for synchronization of magnetic resonance imaging (MRI). *Acta Acust United Ac* 94:148–155
- Becker M, Frauenrath T, Hezel F et al (2010) Comparison of left ventricular function assessment using phonocardiogram- and electrocardiogram-triggered 2D SSFP CINE MR imaging at 1.5T and 3.0T. *Eur Radiol* 20:1344–1355
- Griswold MA, Jakob PM, Chen Q et al (1999) Resolution enhancement in single-shot imaging using simultaneous acquisition of spatial harmonics (SMASH). *Magn Reson Med* 41:1236–1245
- Kellman P, McVeigh ER (2005) Image reconstruction in SNR units: a general method for SNR measurement. *Magn Reson Med* 54:1439–1447
- Cerqueira MD, Weissman NJ, Dilsizian V et al (2002) Standardized myocardial segmentation and nomenclature for tomographic imaging of the heart: a statement for healthcare professionals from the Cardiac Imaging Committee of the Council on Clinical Cardiology of the American Heart Association. *Circulation* 105:539–542
- Sodickson DK, Hardy CJ, Zhu Y et al (2005) Rapid volumetric MRI using parallel imaging with order-of-magnitude accelerations and a 32-element RF coil array: feasibility and implications. *Acad Radiol* 12:626–635